

# Template synthesis and characterization of WO<sub>3</sub>/TiO<sub>2</sub> composite nanotubes

Lifang Cheng, Xingtang Zhang, Bin Liu, Hongzhe Wang, Yuncai Li, Yabin Huang and Zuliang Du<sup>1</sup>

Key Laboratory for Special Functional Materials, Henan University, Kaifeng, People's Republic of China

E-mail: [zld@henu.edu.cn](mailto:zld@henu.edu.cn)

Received 6 December 2004, in final form 30 March 2005

Published 7 June 2005

Online at [stacks.iop.org/Nano/16/1341](http://stacks.iop.org/Nano/16/1341)

## Abstract

Highly ordered WO<sub>3</sub>/TiO<sub>2</sub> composite nanotubes have been successfully prepared by the combination of the sol–gel chemical method and the anodic aluminium oxide (AAO) templating method. The diameter of the WO<sub>3</sub>/TiO<sub>2</sub> composite nanotubes is about 100 nm, which is in good agreement with the pore diameter of the AAO template. The composite nanotubes are composed of mixed oxides of W<sup>6+</sup> and Ti<sup>4+</sup>.

## 1. Introduction

Tungsten oxide is one of the most promising inorganic materials which exhibit excellent electrochromic, photochromic, and gasochromic properties [1, 2], and it has been widely investigated to be used in electrochromic [3, 4], gasochromic [5], solar energy [6], optical modulation, writing–reading–erasing optical devices [7], flat panel displays [8], gas, humidity, and temperature sensors and so forth [9, 10]. It has been known that TiO<sub>2</sub> is an attractive material with excellent photoresponsive properties [11], and some researchers have attempted to improve the colouration performance of WO<sub>3</sub> thin-films by doping TiO<sub>2</sub> [12, 13]. Most of the studies on WO<sub>3</sub>/TiO<sub>2</sub> have been reported on composite thin films, which can be used in photoelectrochromic devices, gas sensors and photocatalysis, etc [14, 15]. However, investigations on nanoarrays of WO<sub>3</sub>/TiO<sub>2</sub> composite are still few, due to lack of preparation methods for such materials, particularly WO<sub>3</sub>/TiO<sub>2</sub> composite nanotubes. Oxide nanotube arrays of materials containing W and Ti are of great interest for their application in a variety of fields such as photocatalysis, chemical sensors, solar cells and so on.

Over the past decades, the synthesis and functionalization of one-dimensional nanostructural materials has become one of the most highly energized research areas [16]. One of the most powerful and now extensively used methods for synthesizing such structures relies on solid-state templates and sol–gel to control the diameter and length of such structures. In particular, this method can yield highly dense nanoscale arrays,

which are favourable for the fabrication of nanosensors or other nanodevices. Anodic aluminium oxide (AAO) has a packed array of columnar hexagonal cells with central, cylindrical, uniformly sized holes ranging from 4 to 200 nm in diameter, pore lengths from 1 to over 100 μm, and pore density in the range from 10<sup>10</sup> to 10<sup>12</sup> cm<sup>-2</sup> [22]. These unique structure properties and their thermal and chemical stability make AAO ideal templates for the fabrication of one-dimensional nanomaterials. Nanostructures (nanowires and nanotubes) of TiO<sub>2</sub> [17], SiO<sub>2</sub> [18, 19], V<sub>2</sub>O<sub>5</sub>, MnO<sub>2</sub>, WO<sub>3</sub> [20, 21] and many other semiconductor materials have been synthesized using such a sol–gel template synthesis strategy. Little use has been made of the sol–gel technique to synthesize composite semiconductor oxide nanotube arrays.

In this paper, we tried to synthesize WO<sub>3</sub>/TiO<sub>2</sub> composite nanotube arrays using sol–gel template methods, and we investigated the microstructure and formation of WO<sub>3</sub>/TiO<sub>2</sub> composites. The results indicated that highly ordered WO<sub>3</sub>/TiO<sub>2</sub> composite nanotubes embedded in the nanochannels of AAO have been obtained.

## 2. Experimental details

WO<sub>3</sub>/TiO<sub>2</sub> composite nanotubes were prepared by using a sol–gel process [23] in the AAO template. 4 g metallic tungsten powder was added to an ice-cooled beaker containing 60 ml of 30% H<sub>2</sub>O<sub>2</sub> solution. After long-time stirring (10 h), the powder dissolved completely and a faint greenish-yellow solution was obtained; then 5 ml tetrabutyl titanate was added directly to the solution under agitation. Pale yellow agglomerates

<sup>1</sup> Author to whom any correspondence should be addressed.

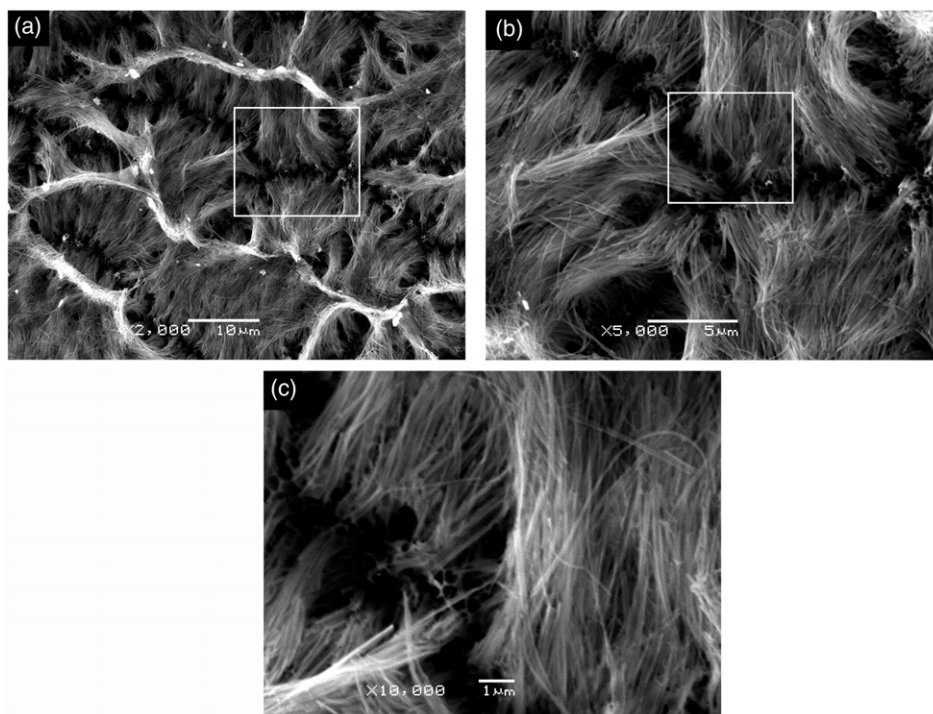


**Figure 1.** SEM images of the  $\text{WO}_3/\text{TiO}_2$  composition nanotubes: (a) large scale, (b) the magnification of a selected region in (a), (c) the magnification of a selected region in (b).

formed instantaneously and floated on the liquid surface. With continued stirring (5 h), the agglomerates dissolved gradually and the solution turned red. After centrifugal sedimentation, a red precursor solution was obtained by removing the insoluble species and then an equal volume of ethanol was added. It could be seen that bubbles were given off from the resulting solution due to the decomposition of excessive hydrogen peroxide. When no further bubbles were observed, the  $\text{WO}_3/\text{TiO}_2$  composite sol was formed and the sol particles were negatively charged. The AAO template (Anopore, Whatman Corporation, UK) was immersed into the sol for 30 min, removed, rinsed with tri-distilled water and placed in air for 30 min. The sol-containing template was heated at  $550^\circ\text{C}$  for 6 h. Finally, the two sides of the products were ground carefully with 1500-mesh sandpaper in order to remove the  $\text{WO}_3/\text{TiO}_2$  composite film deposited on the surface of the AAO template before further characterization. The AAO template was dissolved partly for scanning electron microscopy (SEM, JSM-5600LV equipped with x-ray energy dispersion analysis) observation, and dissolved entirely for transmission electron microscopy (TEM, JEM-100CX) and high-resolution transmission electron microscopy (HRTEM, JEM-2010) observations by a dilute HCl through controlling the reaction time and temperature. For the TEM observation, the  $\text{WO}_3/\text{TiO}_2$  composite nanotubes were dispersed by ultrasonic vibration, and then dropped onto carbon films on copper grids. The chemical composition characterization of the  $\text{WO}_3/\text{TiO}_2$  composite nanotubes was determined by x-ray energy dispersion analysis (EDAX, OXFORD ISIS), x-ray photoelectron spectroscopy (XPS, AXISULTR, with Al  $K\alpha$  x-ray source), and x-ray diffraction (XRD, X'Pert Pro MPD, with Cu  $K\alpha$  radiation).

### 3. Results and discussion

#### *SEM, TEM and HRTEM observation*

SEM images of  $\text{WO}_3/\text{TiO}_2$  composite nanotubes are shown in figures 1(a)–(c). Several clusters of nanotubes can be found in figure 1(a). The clusters may result from the situation in which nanotubes are uncovered from the framework of the AAO template but are not completely freestanding. When the top alumina of the AAO template is dissolved away, the nanotubes embedded in the template are gradually released and inclined to stick together. It is conceivable that the surface energy of the nanotubes causes this interesting phenomenon. Figure 1(a) also shows that the  $\text{WO}_3/\text{TiO}_2$  composite nanotubes prepared are abundant, uniform and highly ordered over a large area. It can be estimated that the length of the  $\text{WO}_3/\text{TiO}_2$  composite nanotubes is more than  $50\ \mu\text{m}$ , which corresponds to the thickness of the AAO template used. Figure 1(b) shows a magnified local image of figure 1(a), and figure 1(c) is a magnified local image of figure 1(b). Figures 1(b), (c) show that the  $\text{WO}_3/\text{TiO}_2$  composite nanotubes are arranged roughly parallel to one another, and are highly uniform in diameter. It can be seen that almost all of the pores are filled.

Figures 2(a), (b) show the TEM images of the  $\text{WO}_3/\text{TiO}_2$  composite nanotubes prepared by immersing the AAO template into the  $\text{WO}_3/\text{TiO}_2$  sol for 30 min at room temperature. Figure 2(a) shows a single nanotube. Figure 2(b) shows multiple nanotubes. It can be seen that the diameter of the nanotubes is about 100 nm, and the same as the pore sizes of the AAO template. In addition, the nanotubes have uniform diffraction contrast, relatively straight morphology and smooth surfaces. As we know, at the pH value used

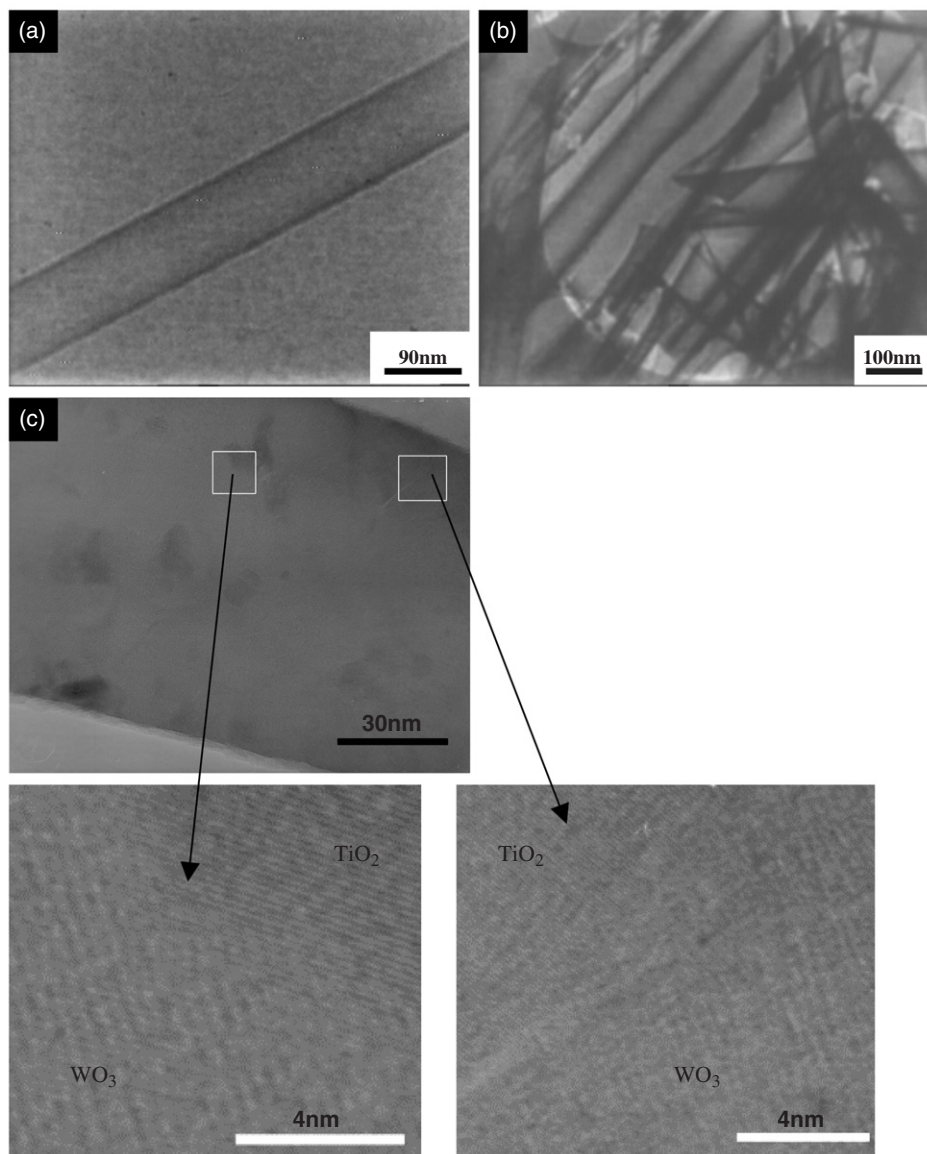


**Figure 2.** ((a), (b)). TEM images of the WO<sub>3</sub>/TiO<sub>2</sub> composition nanotubes obtained by immersing the AAO template into WO<sub>3</sub>/TiO<sub>2</sub> sol: (a) single nanotube, (b) multiple nanotubes. (c) HRTEM image of a WO<sub>3</sub>/TiO<sub>2</sub> composition nanotube.

here the sol particles are negatively charged, although weakly. Meanwhile, the pore walls of the AAO are positively charged, so the WO<sub>3</sub>/TiO<sub>2</sub> composite sol particles are first adsorbed to the surface of the channels of the AAO. Thus, it is not surprising that the WO<sub>3</sub>/TiO<sub>2</sub> composite nanotubes formed, and that single-wall WO<sub>3</sub>/TiO<sub>2</sub> composite nanotubes can be obtained. Solid WO<sub>3</sub>/TiO<sub>2</sub> nanowires will be obtained with long enough immersion times.

The microstructure of the WO<sub>3</sub>/TiO<sub>2</sub> composite nanotubes is investigated using high-resolution transmission electron microscopy (HRTEM). A typical HRTEM image of a single WO<sub>3</sub>/TiO<sub>2</sub> composite nanotube is displayed in figure 2(c). The HRTEM image indicates that the WO<sub>3</sub>/TiO<sub>2</sub> composite nanotubes are composed of numerous single crystals of WO<sub>3</sub> and TiO<sub>2</sub>. It indexed to monoclinic WO<sub>3</sub> single crystals and orthorhombic TiO<sub>2</sub> single crystals. The two images below figure 2(c) are enlarged pictures of the selected regions in figure 2(c) respectively, where the 2-D lattice fringes are

clearly seen. The interplanar spacing is about 0.386 nm, which corresponds to the (002) plane of the monoclinic WO<sub>3</sub>, and the interplanar spacing is about 0.175 nm, which corresponds to the (221) plane of the orthorhombic system of TiO<sub>2</sub>.

#### EDAX, XPS, and XRD analysis

The chemical composition and crystalline structure of the WO<sub>3</sub>/TiO<sub>2</sub> composite nanotubes were determined using XPS, EDAX and XRD. The EDAX spectrum (obtained from SEM with a magnification of 1000 times) of the WO<sub>3</sub>/TiO<sub>2</sub>/AAO composite is shown in figure 3. From this figure, the peaks of W, Ti and O can be clearly seen, indicating that the nanotubes contain Ti, W and O elements. The presence of Al can be ascribed to the remaining AAO membrane.

The XPS spectra of the WO<sub>3</sub>/TiO<sub>2</sub> composite nanotubes are shown in figures 4(a)–(c). These indicate that the WO<sub>3</sub>/TiO<sub>2</sub> composite is formed. Figure 4(a) shows the

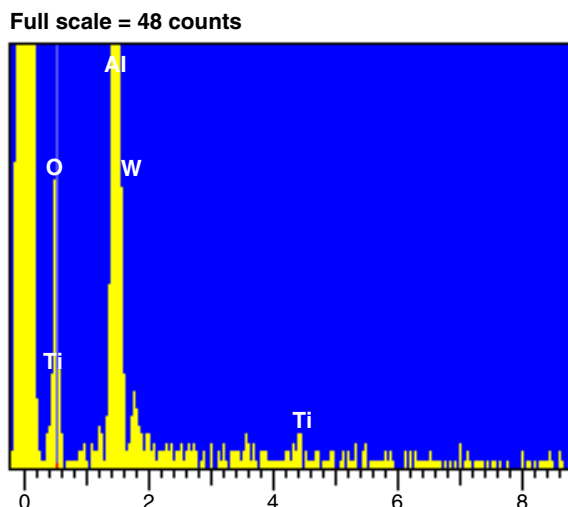


**Figure 3.** EDAX spectrum of the  $\text{WO}_3/\text{TiO}_2/\text{AAO}$  composition. (This figure is in colour only in the electronic version)

binding energy peak of  $\text{O}_{1s}$  at 530.7 eV. Figure 4(b) shows the XPS spectrum of  $\text{W}_{4f}$ . The binding energy peaks located at 35.8 and 37.9 eV are attributed to the spin-orbit splitting of the  $\text{W}_{4f}$  components ( $\text{W}_{4f} 7/2$  and  $\text{W}_{4f} 5/2$ ), which are in good agreement with those of tungsten (VI) trioxide power.

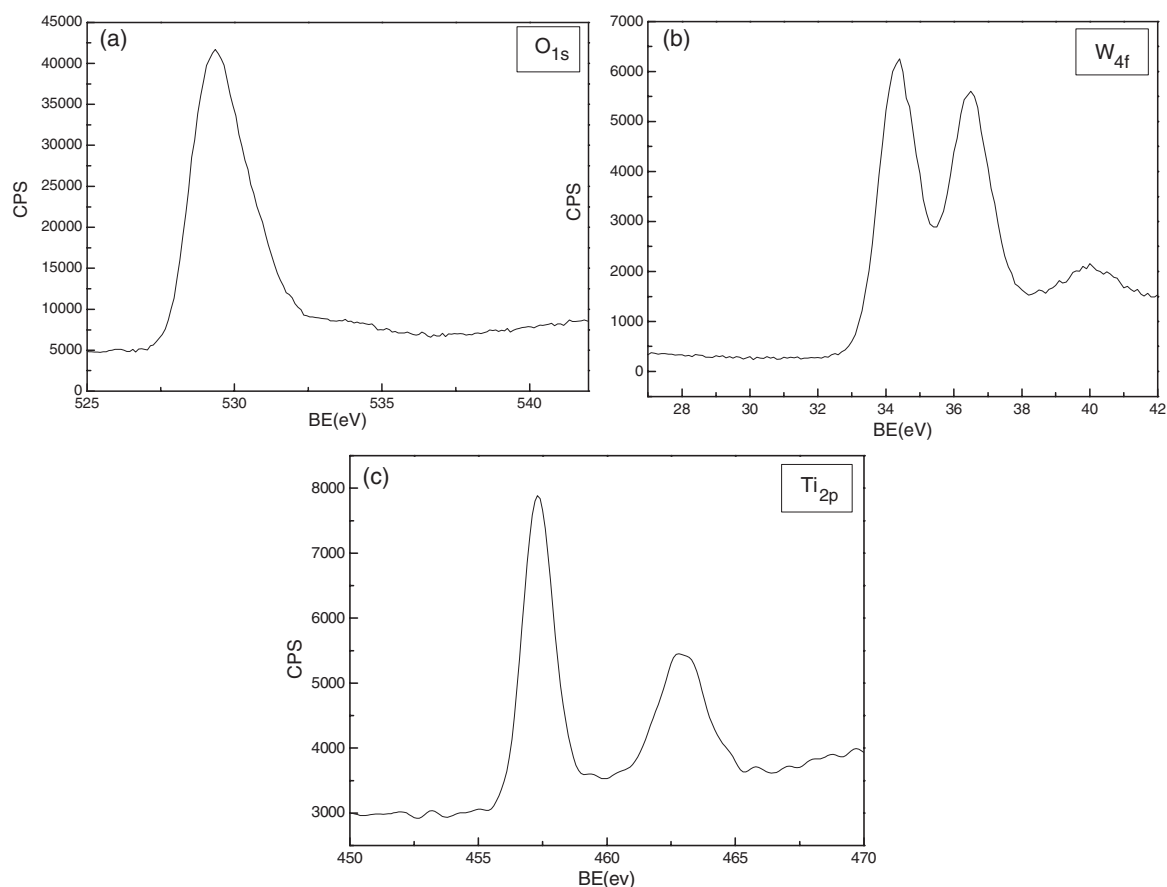


**Figure 4.** XPS spectra of  $\text{O}_{1s}$  (a),  $\text{W}_{4f}$  (b),  $\text{Ti}_{2p}$  (c) at the  $\text{WO}_3/\text{TiO}_2/\text{AAO}$  composition corresponding to the SEM image shown in figure 1.

Figure 4(c) displays the XPS spectrum of  $\text{Ti}_{2p}$ . The peaks located at 458.9 and 464.4 eV are attributed to the spin-orbit splitting of the  $\text{Ti}_{2p}$  components ( $\text{Ti}_{2p} 3/2$  and  $\text{Ti}_{2p} 1/2$ ), which are in good agreement with those of titanium (IV) dioxide power. Therefore, it is evident that the tungsten and titanium in the nanotubes are present in the 6-valent and 4-valent state, respectively.

Figure 5 shows the XRD pattern of the sample within the AAO template prepared at 550 °C. Although background diffraction peaks of  $\text{Al}_2\text{O}_3$  are present, the diffraction peaks at  $\text{WO}_3$  can be observed; the diffraction peaks at 23.15°, 23.61°, 24.37°, 33.30° and 24.19° can be indexed to (002), (020), (200), (022) and (202) of the monoclinic  $\text{WO}_3$  phase, respectively. These peak positions and their relative intensities are in good agreement with the standard diffraction data (JCPDS: 72-1465). However, it can be found that for the composite of  $\text{WO}_3/\text{TiO}_2$  the intensity of the XRD pattern is very weak, and only the XRD peaks of  $\text{WO}_3$  can be observed while none of the peaks of  $\text{TiO}_2$  appears. We think the main reasons are that the particle size remarkably reduces and the grain boundary extremely increases for the  $\text{WO}_3/\text{TiO}_2$  composite. This conclusion was also supported by our comparison experiment, in which the XRD of  $\text{WO}_3/\text{TiO}_2$  composite powder was checked and it was found that the XRD intensity decreased further (data not shown). On the other hand, the mole ratio of  $\text{WO}_3$  and  $\text{TiO}_2$  is about 1 (this can be obtained from the XPS data) but the mass ratio of  $\text{WO}_3$  and

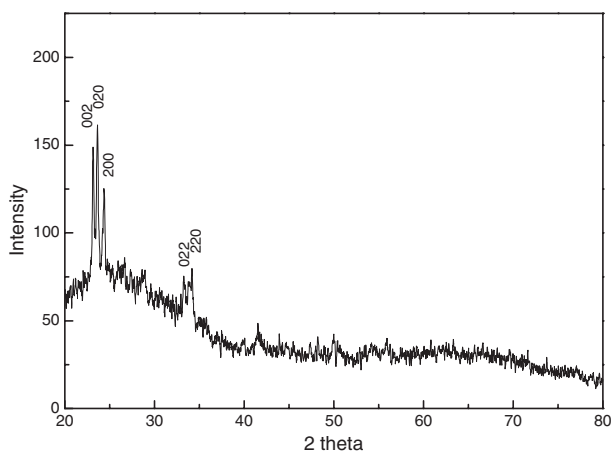


Figure 5. XRD spectrum of the WO<sub>3</sub>/TiO<sub>2</sub>/AAO composition.

TiO<sub>2</sub> is about 5, which resulted in no obvious TiO<sub>2</sub> peaks being observed. The result is in good agreement with earlier work on mixed semiconductor particles [24].

#### 4. Conclusion

In summary, highly ordered WO<sub>3</sub>/TiO<sub>2</sub> composite nanotubes in an AAO template have been prepared successfully using the sol-gel method. XPS and XRD analyses indicate that WO<sub>3</sub>/TiO<sub>2</sub> composite nanotubes are formed. TEM and SEM observations demonstrate that the WO<sub>3</sub>/TiO<sub>2</sub> composite nanotubes are highly ordered, with a diameter of about 100 nm. The mechanism of nanotube growth is also described. The method applied in this work can possibly be used for the preparation of other ordered one-dimensional binary composition semiconductor nanotubes as well.

#### Acknowledgments

This work was supported by the National Natural Science Foundation of China (No. 90306010 and 20371015)

and State Key Basic Research '973' Plan of China (No. 2002CCC02700).

#### References

- [1] Zhuang L, Xu X Q and Shen H 2003 *Surf. Coat. Technol.* **167** 217
- [2] Wang Y D, Chen Z X, Li Y F, Zhou Z L and Wu X H 2001 *Solid-State Electron.* **45** 639
- [3] Özer N 1997 *Thin Solid Films* **304** 310
- [4] Aliev A E and Shin H W 2002 *Solid State Ion.* **154/155** 425
- [5] Shieh J, Feng H M, Hon M H and Juang H Y 2002 *Sensors Actuators B* **86** 75
- [6] Tatsuma T, Saitoh C, Ngaotrakanwivat P, Ohko Y and Fujishima A 2002 *Langmuir* **18** 7777
- [7] Baeck S H, Choi K S, Jaramillo T F, Stucky G D and McFarland E W 2003 *Adv. Mater.* **15** 1269
- [8] Grätzel M 2001 *Nature* **409** 575
- [9] Lee D S, Han S D, Huh J S and Lee D D 1999 *Sensors Actuators B* **60** 57
- [10] Li X L, Liu J F and Li Y D 2003 *Inorg. Chem.* **42** 921
- [11] Song K Y, Park M K, Kwon Y T, Lee H W, Chung W J and Lee W I 2001 *Chem. Mater.* **13** 2349
- [12] Linkous C A, Carter G J, Locuson D B, Ouellette A J, Slattery D K and Smitha L A 2000 *Environ. Sci. Technol.* **34** 4754
- [13] He T, Ma Y, Cao Y A, Hu X L, Liu H M, Zhang G J, Yang W S and Yao J N 2002 *J. Phys. Chem. B* **106** 12670
- [14] Tatsuma T, Saitoh S, Ohko Y and Fujishima A 2001 *Chem. Mater.* **13** 2838
- [15] Miyauchi M, Nakajima A, Watanabe T and Hashimoto K 2002 *Chem. Mater.* **14** 4714
- [16] Ji G B, Tang S L, Xu B L, Gu B X and Du Y W 2003 *Chem. Phys. Lett.* **379** 484
- [17] Lei Y, Zhang L D, Meng G W, Li G H, Zhang X Y, Liang C H, Chen W and Wang S X 2001 *Appl. Phys. Lett.* **78** 1125
- [18] Zhang M, Bando Y, Wada K and Kurashima K 1999 *J. Mater. Sci. Lett.* **18** 1911
- [19] Schlottig F, Textor M, Georgi U and Roewer G 1999 *J. Mater. Sci. Lett.* **18** 599
- [20] Lakshmi B B, Patrissi C J and Martin C R 1997 *Chem. Mater.* **9** 2544
- [21] Lakshmi B B, Dorhout P K and Martin C R 1997 *Chem. Mater.* **9** 857
- [22] Masuda H and Fukuda K 1995 *Science* **268** 1466
- [23] Wang Z C and Hu X F 2001 *Electrochim. Acta* **46** 1951
- [24] Sakthivel S, Geissen S U, Bahnemann D W, Murugesan V and Vogelpohl A 2002 *J. Photochem. Photobiol. A* **148** 283